Time-Resolved Luminescence Biosensor for Continuous Activity Detection of Protein Acetylation-Related Enzymes Based on DNA-Sensitized Terbium(III) Probes

ARTICLE *in* ANALYTICAL CHEMISTRY · AUGUST 2015

Impact Factor: 5.64 · DOI: 10.1021/acs.analchem.5b01338 · Source: PubMed

analytical chemistry

Article

pubs.acs.org/ac

Time-Resolved Luminescence Biosensor for Continuous Activity Detection of Protein Acetylation-Related Enzymes Based on DNA-Sensitized Terbium(III) Probes

Yitao Han, Hao Li, Yufang Hu, Pei Li, Huixia Wang, Zhou Nie,* and Shouzhuo Yao

State Key Laboratory of Chemo/Biosensing and Chemometrics, College of Chemistry and Chemical Engineering, Hunan University, Changsha, 410082, People's Republic of China

Supporting Information

ABSTRACT: Protein acetylation of histone is an essential post-translational modification (PTM) mechanism in epigenetic gene regulation, and its status is reversibly controlled by histone acetyltransferases (HATs) and histone deacetylases (HDACs). Herein, we have developed a sensitive and label-free time-resolved luminescence (TRL) biosensor for continuous detection of enzymatic activity of HATs and HDACs, respectively, based on acetylation-mediated peptide/DNA interaction and Tb^{3+}/DNA luminescent probes. Using guanine (G)-rich DNA-sensitized Tb^{3+} luminescence as the output signal, the polycationic substrate peptides interact with DNA with high affinity and subsequently replace Tb^{3+}, eliminating the luminescent signal. HAT-catalyzed acetylation remarkably reduces the positive charge of the peptides and diminishes the peptide/DNA interaction, resulting in the signal on detection via recovery of DNA-sensitized Tb^{3+} luminescence. With this TRL sensor, HAT (p300) can be sensitively detected with a wide linear range from 0.2 to 100 nM and a low detection limit of 0.05 nM. The proposed sensor was further used to continuously monitor the HAT activity in real time. Additionally, the TRL biosensor was successfully applied to evaluating HAT inhibition by two specific inhibitors, anacardic acid and C464, and satisfactory Z′-factors above 0.73 were obtained. Moreover, this sensor is feasible to continuously monitor the HDAC (Sirt1)-catalyzed deacetylation with a linear range from 0.5 to 500 nM and a detection limit of 0.5 nM. The proposed sensor is a convenient, sensitive, and mix-and-read assay, presenting a promising platform for protein acetylation-targeted epigenetic research and drug discovery.

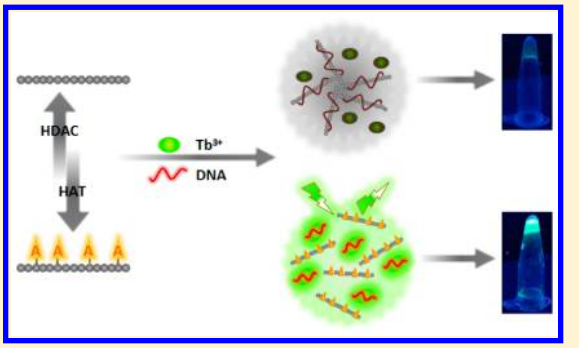

Protein acetylation is a prevalent post-translational modification (PTM) and plays a critical role in the regulation of gene expression, genome stability, mitosis, and nutrient metabolism.[1] Two opposing enzyme classes, histone acetyltransferases (HATs) and histone deacetylases (HDACs), reversibly control the dynamic acetylation of histone proteins, which is an important mechanism for epigenetic modulation of transcription and chromatin structure.[2] HATs transfer the acetyl group from the acetyl-coenzyme A (Ac-CoA) to the positively charged lysine residues on the N-terminus of the histone proteins, producing neutral acetylated lysines (Scheme 1A) and consequently resulting in the decondensation of chromatin structure and the activation of gene expression.[3] The dysfunction of HATs causes the manifestation of several diseases, such as cancers, metabolic syndromes, and neurological disorders.[4] Recently, HDAC inhibitors have emerged as target-selective drugs with epigenetic mechanism to treat rare T-cell lymphomas, hematologic, and solid tumors.[5] Therefore, the potent bioanalytical method for detecting activity of acetylation-related enzymes and screening of their inhibitors will benefit biochemical research and pharmaceutical development.

Conventional assays of HATs and HDACs rely on autoradiography and radio isotopes, which have the drawbacks of radioactive wastes, multistep procedures, and intricate labeled substrates.[6] Hence alternative methods based on fluorescence detection were explored widely as the most typical nonisotopic strategy.[7−12] Several intriguing fluorescent HAT sensors have been developed, such as the quantum dots (QDs)-based immunosensors using the acetyl-specific antibody and peptide-tailed QDs,[8] the acetylation protection assay based on suppression of exopeptidase cleavage by acetylation and superquenching ability of nanomaterials,[9] and the direct measurements of byproduct CoA by exploiting thiol-reactive probes[10] or nucleic acid-mimicking CoA-Au coordination polymer.[11] Schwienhorst's group reported a fluorescent peptide sensor for HDAC detection with the assistance of trypsin digestion.[12] Kikuchi's group developed a series of HDAC fluorescent assays based on dye-tagged peptide probes[13a,b] and tetraphenylethylene-derivative probe,[13c] avoiding the usage of protease. Although the potency of these methods has been

Received: April 9, 2015
Accepted: August 26, 2015

DOI: 10.1021/acs.analchem.5b01338
Anal. Chem. XXXX, XXX, XXX−XXX

Scheme 1. (A) Real-Time Acetylation Is Reversibly Controlled by Histone Acetyltransferases (HATs) and Histone Deacetylases (HDACs). (B) Principle of the TRL Biosensor for Detection of Acetylation-Related Enzymes Activity Based on Guanine-Rich ssDNA-Sensitized Tb^{3+} Probes

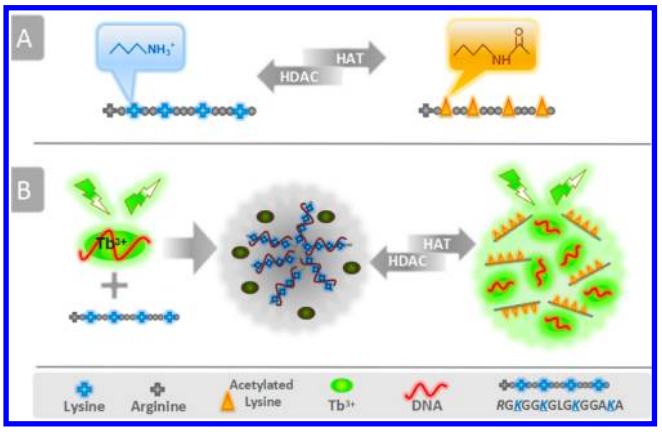

proved, some obstacles still exist. For instance, most of these methods are only applicable for end point detection and unavailable for continuously monitoring the enzymatic activity, and the preparation of fluorescent probes in these methods is usually sophisticated with the covalent labeling of peptides or antibodies. Hence, in order to overcome these obstacles, it is highly desirable to design a new label-free strategy for continuous detection of acetylation-related enzymes activity.

The time-resolved luminescence (TRL) bioassays attracted broad attention since their probes possess unique photophysical properties, such as sharp emission band, large Stokes' shift, and long lifetime.[14] Compared with fluorescence-based assays, TRL strategies can solve the problem of interfering background luminescence because the detection of the luminescence signal is delayed for a certain time following the termination of pulsed excitation and only the long-lived luminescent probes remain visible to the detector.[14] Lanthanide ion complexes are representative long lifetime emitting materials possessing unique luminescent properties due to the 4f orbitals of lanthanide ion.[15] Since the direct excitation of lanthanide ion to luminesce is difficult, the adjacent ligands that strongly absorb in the ultraviolet (UV) region and provide antenna effect are essential for sensitization of lanthanide ion luminescence.[16] On the basis of this fact, various ligands were utilized for the antenna coordination, such as lanthanide ion chelates,[17] cryptates,[18] and lanthanide ion-binding peptides.[19] Recently, the G-rich single-stranded DNA (ssDNA) with guanine-rich sequence have been demonstrated as effective antenna ligands to sensitize the luminescence of terbium ion (Tb^{3+}).[20] Because of the noncovalent interaction between Tb^{3+} and ssDNA, a few simple and label-free DNA sensors have been developed based on ssDNA-sensitized Tb^{3+} luminescence to detect metal ions,[20a] small molecules,[20b] and DNA.[20c] However, to the best of our knowledge, the application of TRL assay to the detection of protein-acetylation-related enzymes is scarce. Since the acetylation of histone proteins removes the positive charges of histone and weakens the interaction between histone and DNA, it is intriguing to develop a biosensing mechanism for HAT/HDAC activity which mimics the protein-acetylation-mediated interaction between histone and DNA. Hence, we envisioned that ssDNA-sensitized Tb^{3+} luminescent probes could provide a label-free TRL strategy for probing peptide acetylation and acetylation-related enzymes activity.

Herein, we describe a sensitive and label-free sensor for continuous detection of acetylation-related enzymes, HAT and HDAC, using G-rich DNA-sensitized Tb^{3+} luminescent probes. Our TRL biosensor is based on the facts that the negatively charged ssDNA is an excellent ligand for binding of cationic peptides through electrostatic interactions, and a G-rich ssDNA has a significant antenna capability for sensitizing the Tb^{3+} emission. Similar to acetylation-mediated histone−DNA interaction, the lysine-acetylation-caused charge change of substrate peptides leads to the different competitiveness between peptides and Tb^{3+} to bind ssDNA, displaying the significant difference of luminescence intensity. This TRL sensor is feasible to continuously monitor the acetylation process by HAT and the deacetylation process by HDAC. Compared with the conventional HAT/HDAC sensors, the proposed TRL sensor presents a new sensing platform for probing HAT and HDAC activity, which overcomes common shortcomings including sophisticated peptide labeling, discontinuous detection, low sensitivity, and intricate sensor composition.

EXPERIMENTAL SECTION

Reagents and Materials. All oligonucleotides were synthesized and purified by Sangon Inc. (Shanghai, China). All peptides were purchased from GL Biochem Ltd. (Shanghai, China). Recombinant GST-purified p300 HAT domain, recombinant N-terminal GST-tagged Sir1 HDAC, acetyl coenzyme A (Ac-CoA), coenzyme A (CoA), β-nicotinamide adenine dinucleotide hydrate (NAD^+), anacradic acid, C646, quinine bisulfate, cAMP-dependent protein kinase A (PKA), casein kinase II (CK2), protein phosphatase 1 (PP1), caspase-3 (Caspase), lysozyme, thrombin, BSA, DNase I, and RNase were purchased from Sigma-Aldrich (Shanghai, China). Stock solutions and serial dilutions of anacardic acid were prepared in anhydrous DMSO and stored at −20 °C before use. All other chemicals of analytical reagent grade were obtained from Changsha Chemical Reagents Company (Changsha, China) and used as received without further purification. All solutions were prepared using ultrapure water (18.3 MΩ cm) from the Millipore Milli-Q system.

Instrumentation. Luminescence and fluorescence measurements were performed on the QuantaMasterTM4 fluorescence spectrometer (PTI, London, Canada). For the TRL spectra, a delay time of 500 μs and a gate time of 1 ms were used, all samples were illuminated at an excitation wavelength of 290 nm, the luminescence emission was scanned from 480 to 650 nm, and the slit width was 20 nm. For fluorescence measurement, the excitation wavelength used was 485 nm, the emission spectrum was from 500 to 650 nm, and the slit width was 5 nm. Except for the specific cases mentioned in the text, the luminescence and fluorescence intensities of all of the spectra were measured at 546 and 512 nm, respectively, which were the maximum emission peaks. Every measurement was repeated three times by triplicate enzymatic reactions under the same condition (n = 3). The pictures of luminescent samples were taken using the WFH-204B hand-held UV lamp (Shanghai, China).

Discrimination of Acetylated Peptide from Substrate Peptide by Tb^{3+}/ssDNA Probe. The typical luminescent probe of Tb^{3+}/ssDNA was prepared in a 100 μL mixture containing 40 nt polyG ssDNA (G40, 1 μM), Tb^{3+} (5 μM), and

DOI: 10.1021/acs.analchem.5b01338
Anal. Chem. XXXX, XXX, XXX−XXX

10 mM Tris-HCl (pH 7.4). The mixture was incubated for 1 min at room temperature. The preprepared Tb^{3+}/ssDNA probe was further incubated with the substrate peptide P (RGKGGKGLGKGGAKA) (1 μM) or the completely acetylated peptide P(Ac) (RGKGGKGLGKGGAKA, the underlines indicating the acetylated sites) (1 μM) for 1 min. Then, the TRL excited at 290 nm was recorded. The optimization of the Tb^{3+}/ssDNA probe was performed by using a series of DNA oligos with different base compositions (polyA, polyT, polyC, and polyG ssDNA) and lengths (length of polyG ssDNA from 20 to 60 nt). Here polyG was defined as (GGGGA)n, including one adenine after every four guanines, because of the limitation of DNA synthesis. The effect of the peptides with different acetylation extents on the luminescence signal of Tb^{3+}/ssDNA probe was investigated by exploiting the peptides P, P(1) (RGKGGKGLGKGGAKA), P(2) (RGKGGKGLGKGGAKA), P(3) (RGKGGKGLGKGGAKA), and P(Ac).

Detection of HAT Activity Based on TRL Sensor. HAT p300 (100 nM) was incubated with the substrate peptide P (1 μM), acetyl-CoA (10 μM) or CoA (10 μM), and Tb^{3+}/ssDNA probe (1 μM) in the HAT reaction buffer with a total volume of 100 μL at 30 °C for 50 min. Then the mixture solution was taken out for luminescence measurement. For the quantitative detection, a range of concentrations (0−1000 nM) of p300 was investigated.

For the continuous detection, a sample containing Tb^{3+}/ssDNA probe (1 μM) and the substrate peptide P (1 μM) in the HAT reaction buffer with a total volume of 80 μL was loaded into the spectrometer cuvette and then p300 (final concentration, 100 nM) and acetyl-CoA (final concentration, 10 μM) were added to this cuvette quickly. At the same time, the mixture solution was measured immediately for continuous luminescence detection from 0 to 240 min at 546 nm under continuous stirring at 30 °C.

For the time-point detection, a sample containing the Tb^{3+}/ssDNA probe (1 μM) and the substrate peptide P (1 μM) was incubated with p300 (100 nM) and acetyl-CoA (10 μM) in the HAT reaction buffer with a total volume of 100 μL at 30 °C for different times (0−240 min). Then each sample was taken out at a specific reaction time point for luminescence measurement.

Detection of HDAC Activity Based on TRL Sensor. HDAC Sirt1 (400 nM) was incubated with the acetylated substrate peptide P(Ac) (1 μM), NAD^+ (200 μM), and Tb^{3+}/ssDNA probe (1 μM) in the HDAC reaction buffer with a total volume of 100 μL at 30 °C for 60 min. Then the mixture solution was taken out for luminescence measurement. For the quantitative detection, a range of concentrations (0−1000 nM) of Sirt1 was investigated.

For the continuous detection, a sample containing a Tb^{3+}/ssDNA probe (1 μM) and the acetylated substrate peptide P(Ac) (1 μM) in the HDAC reaction buffer with a total volume of 80 μL was loaded into the spectrometer cuvette and then Sirt1 (final concentration, 400 nM) and NAD^+ (final concentration, 200 μM) were added to this cuvette quickly. At the same time, the mixture solution was measured immediately for continuous luminescence detection from 0 to 240 min at 546 nm under continuous stirring at 30 °C.

Supporting Information (SI) contains the experimental details of the estimation of quantum yield, the luminescence lifetime, and the dissociation constants, the detection of HAT inhibitors based on the TRL sensor, Z'-factor calculation, the influence of some interfering biomolecules existing in biological systems on the signal of TRL biosensor, HeLa cell culture and lysate preparation, the detection of HAT activity by the TRL biosensor in the cell lysate, the discrimination of acetylated peptide from substrate peptide by the FITC-tagged peptide/ssDNA fluorescent probe, and the detection of HAT and HDAC activity based on the fluorescent sensor.

RESULTS AND DISCUSSION

Detection Principle of Tb^{3+}/DNA-Based TRL HAT Sensor. Relying on the Tb^{3+}/ssDNA complex-based luminescent probe and DNA condensation by the positively charged substrate, we proposed a novel label-free sensor for the continuous monitoring of acetylation-related enzymes activity, which is schematically illustrated in Scheme 1. Guanine can greatly enhance the Tb^{3+} emission because its triplet energy state overlaps with the resonance energy levels of Tb^{3+};[20] thus G-rich ssDNA was employed as the sensitization ligands of Tb^{3+} to form a luminescent Tb^{3+}/ssDNA probe. Since the polycationic substrate peptide of HAT has stronger electrostatic affinity to G-rich ssDNA than Tb^{3+}, the substrate peptide can form the stable complexes with polyanionic ssDNA (peptide/ssDNA) and replace Tb^{3+} which is originally coordinated with ssDNA. Then Tb^{3+} is released and the luminescence, correspondingly, is effectively quenched. However, after acetylation by HAT, the resulting acetylated peptides significantly remove their positive charges, causing the peptide/ssDNA complexes dissociation and the release of ssDNA, followed by the recoordination of ssDNA and Tb^{3+}. Thereby, the intermolecular energy transfer from the antenna ligand ssDNA to Tb^{3+} is restored, and the long-lived Tb^{3+} luminescence is turned on (Scheme 1B). Hence, the acetylation-mediated Tb^{3+} luminescence switch could be used to measure acetylation-related enzymes.

Guanine-Rich ssDNA-Sensitized Luminescence of Tb^{3+}. We first investigated the luminescence of the Tb^{3+}/ssDNA probe. As exhibited in SI Figure S1, the sole Tb^{3+} or G-rich ssDNA oligos (40 nt poly G ssDNA, namely, G40) solution showed a very weak luminescence emission under excitation with 290 nm light; however, after Tb^{3+} was incubated with G-rich ssDNA, the four typical characteristic emission peaks of Tb^{3+} appeared at 491, 546, 585, and 620 nm and there was a 160-fold sensitizing enhancement of the luminescent response at 546 nm due to energy transfer from ssDNA to Tb^{3+}. The emission quantum yield of 5 μM Tb^{3+} with 1 μM G40 ssDNA was measured to be 0.029, relative to a standard solution of quinine bisulfate (0.1 N H_2SO_4).[20c] Meanwhile, this luminescent phenomenon can be directly observed by naked eyes under a UV lamp (Figure 1C), and the Tb^{3+}/ssDNA mixture showed a bright green luminescence. Figure 1A shows that the luminescence lifetime of the Tb^{3+}/G-rich ssDNA complex was 0.526 ms, much greater than the lifetime of Tb^{3+} without ssDNA (0.022 ms),[20a,21] suggesting the efficient protection of Tb^{3+} by ssDNA ligand against the nonradiative deactivation via O−H vibration of coordinated H_2O molecules and the energy loss of the Tb^{3+} complex. In order to optimize DNA ligand for effective sensitizing luminescence, a series of DNA oligos with various base contents and lengths were investigated. The study of different DNA base contents (SI Figure S2A) shows that polyA, polyT, and polyC ssDNA did not increase the emission of Tb^{3+} and only polyG displayed efficient sensitization of luminescence. The unique sensitization effect of G-rich ssDNA is probably due to both the phosphate group and the O6 and N7 atoms of the guanine base

DOI: 10.1021/acs.analchem.5b01338
Anal. Chem. XXXX, XXX, XXX−XXX

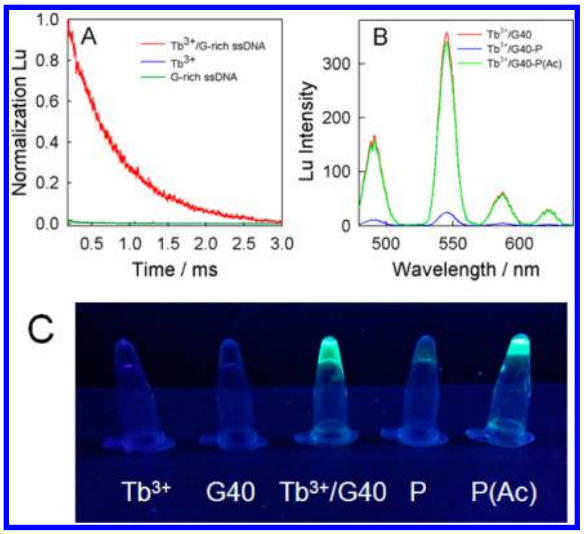

Figure 1. (A) Luminescence lifetime of the sole Tb^{3+}, sole G-rich ssDNA oligos (G40), and their mixture. (B) Luminescence responses of the Tb^{3+}/G40 probe in the presence of substrate peptide (P) or its acetylated product P(Ac). (C) Corresponding luminescence emission of the sole 10 μM Tb^{3+}, sole 2 μM G40, and the Tb^{3+}/G40 probe in the presence of 2 μM P or 2 μM P(Ac) under a UV lamp with 254 nm excitation wavelength.

synchronously coordinating with Tb^{3+}, thus increasing the binding affinity and promoting efficient intermolecular energy transfer from guanine to Tb^{3+}.[20c] Further investigation concerning the length of the ssDNA probe (SI Figure S2B) showed that the luminescence response sharply increased with increasing length of polyG ssDNA from 20 to 40 followed by a gentle increase when the sequence was longer than 40. Therefore, after the comprehensive consideration of the optimization results and the costs of nucleic acids, G40 was exploited as the probe in the following experiments.

Discrimination of Acetylated Peptide from Substrate Peptide by Tb^{3+}/ssDNA Probe. Our acetylation sensing mechanism is based on the acetylation-mediated peptide/DNA interaction, which mimics the protein-acetylation-regulated histone/DNA interaction in the cell nucleus.[1−3] The lysine acetylation of the substrate peptide remarkably reduces its positive charges; thus the substrate peptide and its acetylated form showed different capability to bind ssDNA and displace Tb^{3+}. The substrate peptide P is 15 amino acids (aa)-long and it carries five positive charges which is derived from the N-terminal tail of histone H4. Its completely acetylated counterpart P(Ac) contains four acetyl-Lys sites with only one positive charge, representing the expected product of HAT. As illustrated in Figure 1B, the incubation of P with Tb^{3+}/G40 probe significantly quenched the luminescence of Tb^{3+} (up to 93%), while the luminescence of the Tb^{3+}/G40 probe almost unchanged after P(Ac) treatment. The luminescence signal of the Tb^{3+}/G40 probe to P(Ac) is 13.6 times that to P, indicating the proposed sensor can effectively distinguish between P and P(Ac). Meanwhile, acetylated P(Ac) can be well discriminated from unacetylated P via direct visualization by naked eyes observation with a UV lamp (Figure 1C). These results are probably attributed to the remarkable reduction of positive charges (from five to one) by acetylation (from P to P(Ac)) that significantly weakens the electrostatic interactions between peptides and ssDNA.

We further assessed the binding affinities between P and G40 ssDNA, P(Ac) and G40 ssDNA, and Tb^{3+} and G40 ssDNA, respectively. Both P and P(Ac) are polycationic and capable of condensing DNA to yield polyionic complex at a specific concentration. Hence we employed FITC-tagged peptides (F−P) to measure their interaction with ssDNA since the formation of peptide/ssDNA polyionic complex brings the FITC-tagged peptide proximate and induces the fluorescence self-quenching of FITC.[13a,22,23] FITC-tagged F−P or F−P(Ac) was used for fluorescence titration with G40 ssDNA. As shown in SI Figure S3A, the fluorescence intensity of F−P gradually decreased as the concentration of G40 increased, while that of F−P(Ac) declined slowly. According to the titration curves, the apparent dissociation constant values (K_d) of P/G40 and P(Ac)/G40 are 37.6 ± 1.0 nM and 15.1 ± 0.8 μM, respectively, which were estimated by using nonlinear least-squares curve fitting analysis[24] (as shown in the Supporting Information). The binding affinity of Tb^{3+}/G40 ssDNA was estimated from the direct measurement of DNA concentration-dependent luminescence enhancement of Tb^{3+} (shown in SI Figure S3B). The calculated K_d for Tb^{3+}/G40 complex was 1.46 ± 0.08 μM, which is about 40-fold higher than that of P/G40 and around 10 times lower than that of P(Ac)/G40. The order of binding affinity with DNA, P(Ac) < Tb^{3+} < P, strongly testifies that P can efficiently displace Tb^{3+} to bind with DNA but P(Ac) cannot, which solidly supports our acetylation sensing mechanism.

Next, we examined the effect of the peptides with different acetylation extents on the luminescence signal of Tb^{3+}/ssDNA probe (SI Figure S4). The tested peptides, including P(1), P(2), P(3), and P(Ac), containing increasing amounts of acetyl-Lys sites from 1 to 4 cause the luminescence signals which are 3.6, 7.3, 11, and 14 times that of the unacetylated P, implying that the more complete acetylation leads to the better recovery of the luminescence intensity. These results demonstrated that Tb^{3+}/ssDNA probe was able to discriminate peptides with different acetylation extents. Furthermore, we optimized the concentration ratio of peptides/G40 and Tb^{3+}/G40. As illustrated in SI Figure S3, the most significant difference of fluorescence signal between F−P and F−P(Ac) and the maximal luminescence of Tb^{3+} with G40 were obtained at 1:1 (peptides/G40) and 1:5 (Tb^{3+}/G40) molar ratio (red dotted line), respectively. Additionally, the luminescence intensity of Tb^{3+} was measured in the presence of all of the species used in the following experiment, including the peptides (P and P(Ac)), acetylation-related enzymes (HAT p300 and HDAC Sirt1), and their cosubstrates (Ac-CoA and NAD^+). As shown in SI Figure S5, except G40 ssDNA, all of the other species cannot sensitize the luminescence of Tb^{3+}. The addition order of Tb^{3+} and peptides was also discussed (SI Figure S6). Regardless of whether Tb^{3+} was added prior to peptides or with the reversed order, the comparable luminescence quenching was observed. Hence, the sequential addition of Tb^{3+} and peptides was performed in our assay, providing a potential platform for continuous detection.

The time-resolved feature of the TRL sensor provides the superb anti-interference ability against background luminescence. To prove this advantage, we challenged the TRL sensors with FAM, a fluorescent dye whose emission spectrum largely overlaps with that of Tb^{3+}/DNA complex, as the coexisting interference (SI Figure S7). The coexisting FAM shows negligible effect on the TRL signals in response to either P or P(Ac), indicating that the longer lifetime of DNA-sensitized

DOI: 10.1021/acs.analchem.5b01338
Anal. Chem. XXXX, XXX, XXX−XXX

luminescence of Tb^{3+} provided an opportunity to eliminate any interference from autofluorescence and other background within the sample, increasing the specificity and signal-to-noise for detection.

Detection of HAT Activity Based on TRL Sensor. Figure 2A shows typical luminescence detection of HAT activity by

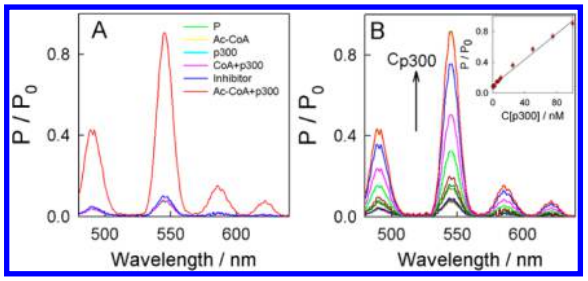

Figure 2. TRL HAT sensor based on a Tb^{3+}/G40 probe. (A) Response of the TRL sensor to sole p300, sole Ac-CoA, coexistence of p300 and CoA, p300-specific inhibitor (anacardic acid), and coexistence of p300 and Ac-CoA. (B) Luminescent response of the Tb^{3+}/G40-based TRL sensor to various concentrations of p300 (from bottom to top: 0, 0.1, 0.2, 0.5, 1.0, 2.5, 5.0, 7.5, 10, 25, 50, 75, 100, 500, and 1000 nM) and its calibration curve (inset).

our Tb^{3+}/G40 probe. The transcriptional activator protein p300 was exploited as a model HAT enzyme for investigation. Upon the reaction of P with p300 and the cosubstrate Ac-CoA, the luminescence of the sensor significantly increased with about 91% recovery of the luminescence intensity (shown in Figure 2A). The control samples, including sole p300 or Ac-CoA, and the coexistence of p300 and CoA showed unchanged luminescence relative to the background. Addition of HAT-specific inhibitor (anacardic acid) completely inhibited the luminescence enhancement, indicating that the HAT-catalyzed acetylation caused a significant signal change. Figure 2B showed that the luminescence response at 546 nm of the Tb^{3+}/G40 HAT sensor increased gradually as the concentrations of p300 increased and the inset of Figure 2B illustrated the linear luminescence responses of the proposed sensor. The linear range was from 0.2 to 100 nM with a regression coefficient (R) of 0.995 and the detection limit (DL) was as low as 0.05 nM (S/N = 3), which were superior or comparable to those of previously reported HAT (p300) assays (detailed comparison shown in SI Table S1).[8,9,11]

Furthermore, the TRL assay was successfully exploited to dynamically monitor acetylation levels of substrate peptides in real time. The luminescence emission at 546 nm was continuously measured from 0 min after the start of acetylation by addition of p300 and Ac-CoA into a sample containing P and the Tb^{3+}/G40 probe. Figure 3 exhibited that the luminescence of Tb^{3+}/G40 probe gradually increased after the addition of 100 nM p300 and 10 μM Ac-CoA, until it reached saturation at 50 min approximately (red dotted line), confirming that our Tb^{3+}-based TRL biosensor is feasible for continuously monitoring HAT activity. In addition, we monitored the enzyme reactions using a time-point assay. As displayed in SI Figure S8, the acetylation reaction catalyzed by p300 HAT was investigated at specific reaction time points. After addition of p300 and Ac-CoA into the sample containing the Tb^{3+}/G40 probe and substrate peptide, the luminescence signal increased and reached a plateau in 50 min, which was consistent with the continuous assay.

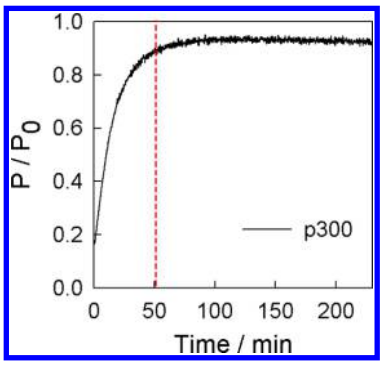

Figure 3. Continuous investigation of the luminescence response of the Tb^{3+}/G40 probe to peptide acetylation in the presence of p300 and Ac-CoA at 546 nm from 0 to 240 min. The red dotted line shows that the luminescence intensity recovered 90%.

Histone acetyltransferase plays a critical role in eukaryotic regulation of gene expression, metabolism, and other key cellular functions.[1−3] Thus, we attempted to test the feasibility of the proposed TRL-based biosensor in complex settings, such as cell lysate samples. We first investigated the influence of some biomolecules generally existing in biological systems on the signal of our proposed HAT sensor, such as proteins, amino acids, DNA, and RNA. As shown in SI Figures S9 and S10, seven nonspecific proteins and 20 standard proteinogenic amino acids show no obvious influence on the HAT detection of our sensor, but the presence of DNA or RNA significantly influences the signals of both the substrate peptide and the acetylated product since the coexisting DNA or RNA not only compete with the G40 probe to bind Tb^{3+} but also influence the interaction between the G40 probe with peptides (SI Figure S11). However, we found that the interference of DNA/RNA can be remarkably eliminated by DNase I/RNase treatment which removes coexisting DNA/RNA before the addition of Tb^{3+}/G40 DNA probe (the detailed experimental processes and discussion are shown in the SI). After thorough assessment of the effects of the potential interfering biomolecules, we attempted to use our TRL biosensor for detection of HAT activity in the diluted Hela cell lysate samples (30,000 cells/mL) spiked with 100 nM HAT p300. As shown in SI Figure S12, taking advantage of DNase I/RNase treatment to remove cellular DNA/RNA, the interference of the diluted cell lysate was evidently alleviated and the peptides before and after HAT catalysis can be efficiently discriminated. We further found that the HAT enzymatic reaction and the DNase I/RNase treatment can be carried out simultaneously, indicating that the DNase I/RNase treatment would not extend the total detection time. However, when the cell concentration was higher than 30,000 cells/mL (shown in SI Figure S13), the capacity of the TRL assay to discriminate the acetylated product from substrate peptide was significantly attenuated, despite the treatment of cell lysate by the DNase I/RNase, which indicated that high-concentration cell lysate shows remarkabe influence on the performance of our HAT sensor. This phenomena probably resulted from the high concentration of some biomacromolecules and small molecules with highly negative charges or strong chelating property in crude cell lysate greatly interfering with the electrostatic interaction between peptide and DNA and the chelation between Tb^{3+} and DNA. Hence this TRL HAT sensor might be applicable in diluted cell lysate samples with low concentration (3×10^4 cells/mL) but still has a limitation in high-concentration cell lysate samples.

DOI: 10.1021/acs.analchem.5b01338
Anal. Chem. XXXX, XXX, XXX−XXX

Detection of Inhibitors for HAT Based on TRL Sensor. The sensitive screening methods for HATs inhibitors are crucial for pharmaceutical development.[4] Anacardic acid and C646, two potent HAT inhibitors, were selected to test the feasibility of our sensor in inhibitors screening.[25] Figure 4

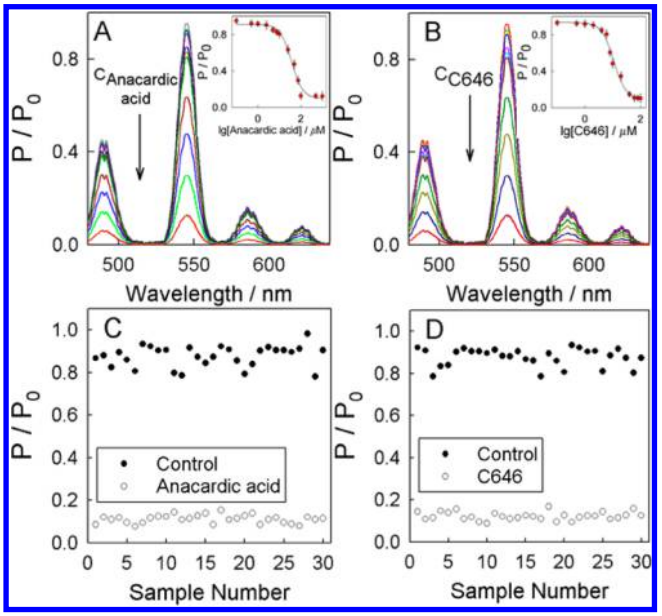

Figure 4. Detection of HAT inhibition based on the TRL sensor. Various concentrations of anacardic acid (A) or C646 (B) were used for investigation of HAT inhibition. From top to bottom: anacardic acid, 0, 0.1, 0.5, 1.0, 2.5, 5.0, 7.5, 10, 25, 50, 75, 100, 500, and 1000 μM; C646, 0.1, 0.5, 1.0, 2.0, 4.0, 6.0, 8.0, 10, 20, 40, 60, 80, and 100 μM. Inset shows the luminescence signal curve as a function of the concentration of HAT inhibitors. Evaluation of this Tb^{3+}/G40-based luminescent approach for high-throughput screening of 100 μM anacardic acid (C) or 60 μM C646 (D).

depicts that the luminescence signal of the sensor decreased with the increasing concentration of two inhibitors, showing that p300 was inhibited. When the luminescence response as a function of the concentration of each inhibitor was plotted, a sigmoidal profile was observed from the insets of Figure 4A,B. The corresponding IC_{50} value (the concentration of the inhibitor leading to the half-maximal inhibition of the enzyme activity) of anacardic acid and C464 toward p300 was estimated to be 53 and 9.4 μM, respectively. The results proved that C464 is of five times higher potency than anacardic acid, which is comparable to those reported previously.[26] Hence, this proposed sensor is feasible in the analysis and screening of small-molecule inhibitors. Furthermore, the robustness and reproducibility of this Tb^{3+}/ssDNA-based TRL approach were evaluated to determine if this sensor would be appropriate for usage in a high-throughput screening (HTS) assay. The Z'-factor is an available criterium to quantify the suitability of a particular assay for use in a full-scale, high-throughput screening.[27] In general, the acceptable value of Z'-factor should be between 0.5 and 1 for an assay to be considered appropriated for HTS, as assays with a Z'-factor in this range exhibit large dynamic ranges and wide separation of positive and negative results. As shown in Figure 4C,D, the Z'-factors of anacardic acid and C646 were 0.73 and 0.76, respectively, indicating that this method would be a solid strategy with good reproducibility for HTS assays in practice.

Detection of HDAC Activity Based on TRL Sensor. Furthermore, whether the deacetylation process catalyzed by HDAC can be detected by the TRL biosensor was explored. Sirt1 is a class III (sirtuin family) HDAC, and its function requires NAD^+ as a cofactor. It is known that Sirt1 is involved in metabolism, aging, and age-related diseases such as cancer.[13] Here Sirt1 activity was measured using the Tb^{3+}/G40 probe. As exhibited in Figure 5A, the substrate peptide P(Ac)

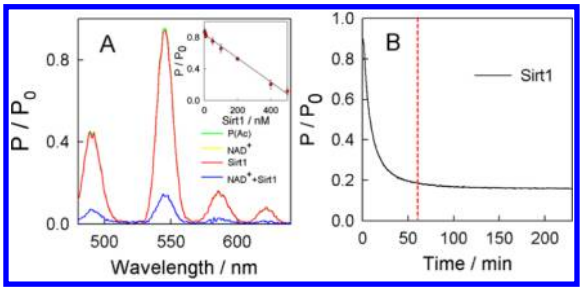

Figure 5. TRL HDAC sensor based on the Tb^{3+}/G40 probe. (A) Response of the TRL sensor to sole NAD^+, sole Sirt1, and coexistence of NAD^+ and Sirt1. Inset shows the luminescence signal curve as a function of the concentration of Sirt1. (B) Continuous investigation of the luminescence response of the Tb^{3+}/G40 probe to deacetylation in the presence of NAD^+ and Sirt1 at 546 nm from 0 to 240 min. The red dotted line shows that the luminescence intensity decreased to 18%.

deacetylated by Sirt1 with NAD^+ showed decreased luminescence, whereas each reactant alone exhibited negligible signal change, implying that the TRL biosensor was feasible for probing HDAC activity as well. The calibration curve of signal ratios versus the Sirt1 concentration was plotted in the inset of Figure 5A. The linear range was from 2 to 500 nM with a detection limit of 0.5 nM (S/N = 3), and the regression coefficient R was 0.996. Subsequently, the continuous detection of deacetylation reaction was investigated (Figure 5B). The luminescence intensity at 546 nm continuously decreased after addition of 400 nM Sirt1 and 200 μM NAD^+ to start deacetylation and reached a platform at approximately 60 min (red dotted line). Therefore, we proved that the Tb^{3+}/ssDNA-based TRL sensor is an effective approach for evaluating the activity of HAT and HDAC in the regulation of reversible protein acetylation.

Meanwhile, for comparison, we have developed a counterpart fluorescent HAT/HDAC sensor based on a similar peptide/ssDNA system and FITC-tagged substrate peptide. The detailed design and analytical performances of this fluorescent sensor are shown in the Supporting Information. Compared with its fluorescent counterpart, the Tb^{3+}-based TRL sensor showed better analytical performance because of its excellent anti-interference capability and long emission lifetime.

CONCLUSIONS

In summary, we reported a novel and label-free biosensing platform for continuous detection of acetylation-related enzymes activity using Tb^{3+}/ssDNA-based luminescent probes. The acetylation of the peptide probe significantly alters its intrinsic charges and subsequently regulates its capability to bind with G-rich ssDNA and replace Tb^{3+}, resulting in the significant change of ssDNA-sensitized Tb^{3+} luminescence signals to reflect enzymatic activity of HAT or HDAC. This facile strategy has several advantages over conventional HAT and HDAC assays: (1) this system directly monitors the

DOI: 10.1021/acs.analchem.5b01338
Anal. Chem. XXXX, XXX, XXX−XXX

enzymatic activity, enabling the continuous analysis of the enzymatic reaction; (2) our assay is label-free and avoids the complicated bioconjugation and immobilization of antibody or fluorophore; (3) our HAT assay is a rapid, mix-and-read, and turn on procedure that can also be exploited for the high-throughput screening of HAT inhibitors. We expect this TRL sensing system could form a generic biosensing platform for HATs and HDACs with its potential utility for anti-carcinogenic drug discovery.

■ ASSOCIATED CONTENT

Supporting Information

The Supporting Information is available free of charge on the ACS Publications website at DOI: 10.1021/acs.analchem.5b01338.

Additional information including additional experimental section and extensive figures as noted in text (PDF)

■ AUTHOR INFORMATION

Corresponding Author

*Phone: +86-731-88821626. Fax: +86-731-88821848. E-mail: niezhou.hnu@gmail.com.

Notes

The authors declare no competing financial interest.

■ ACKNOWLEDGMENTS

This work was financially supported by the National Natural Science Foundation of China (Grant Nos. 21222507, 21175036, 21235002, and 21475038), the National Basic Research Program of China (973 Program, Grant No. 2011CB911002), the Foundation for Innovative Research Groups of NSFC (Grant 21221003), and the Ph.D. Programs Foundation of the Ministry of Education of China (Grant No. 20120161110025).

■ REFERENCES

(1) Jenuwein, T.; Allis, C. D. *Science* **2001**, *293*, 1074−1080.
(2) Marmorstein, R. J. *J. Mol. Biol.* **2001**, *311*, 433−444.
(3) (a) Biel, M.; Wascholowski, V.; Giannis, A. *Angew. Chem.* **2005**, *117*, 3248−3280. (b) Biel, M.; Wascholowski, V.; Giannis, A. *Angew. Chem., Int. Ed.* **2005**, *44*, 3186−3216.
(4) Dekker, F. J.; Haisma, H. J. *Drug Discovery Today* **2009**, *14*, 942−948.
(5) Ratner, M. *Nat. Biotechnol.* **2014**, *32*, 853−854.
(6) (a) Ait-Si-Ali, S.; Ramirez, S.; Robin, P.; Trouche, D.; Harel-Bellan, A. *Nucleic Acids Res.* **1998**, *26*, 3869. (b) Poveda, A.; Sendra, R. *Anal. Biochem.* **2008**, *383*, 296−300.
(7) Yang, Y. Y.; Hang, H. C. *ChemBioChem* **2011**, *12*, 314−322.
(8) Ghadiali, J. E.; Lowe, S. B.; Stevens, M. M. *Angew. Chem., Int. Ed.* **2011**, *50*, 3417−3420.
(9) Han, Y. T.; Li, P.; Xu, Y. T.; Li, H.; Song, Z. L.; Nie, Z.; Chen, Z.; Yao, S. Z. *Small* **2015**, *11*, 877−885.
(10) (a) Kim, Y.; Tanner, K. G.; Denu, J. M. *Anal. Biochem.* **2000**, *280*, 308−314. (b) Trievel, R. C.; Li, F. Y.; Marmorstein, R. *Anal. Biochem.* **2000**, *287*, 319−328.
(11) Chen, S. Y.; Li, Y.; Hu, Y. F.; Han, Y. T.; Huang, Y.; Nie, Z.; Yao, S. Z. *Chem. Commun.* **2015**, *51*, 4469−4473.
(12) (a) Wegener, D.; Hildmann, C.; Riester, D.; Schwienhorst, A. *Anal. Biochem.* **2003**, *321*, 202−208. (b) Wegener, D.; Wirsching, F.; Riester, D.; Schwienhorst, A. *Chem. Biol.* **2003**, *10*, 61−68.
(13) (a) Minoshima, M.; Matsumoto, T.; Kikuchi, K. *Anal. Chem.* **2014**, *86*, 7925−7930. (b) Baba, R.; Hori, Y.; Mizukami, S.; Kikuchi, K. *J. Am. Chem. Soc.* **2012**, *134*, 14310−14313. (c) Dhara, K.; Hori, Y.; Baba, R.; Kikuchi, K. *Chem. Commun.* **2012**, *48*, 11534−11536.
(14) Lu, Y.; Xi, P.; Piper, J. A.; Huo, Y.; Jin, D. *Sci. Rep.* **2012**, *2*, 837.
(15) Bünzli, J. C. *Chem. Rev.* **2010**, *110*, 2729−2755.
(16) Akiba, H.; Sumaoka, J.; Komiyama, M. *ChemBioChem* **2009**, *10*, 1773−1776.
(17) (a) Matsumoto, K.; Nojima, T.; Sano, H.; Majima, K. *Macromol. Symp.* **2002**, *186*, 117−121. (b) Purdy, M. D.; Ge, P.; Chen, J.; Selvin, P. R.; Wiener, M. C. *Acta Crystallogr., Sect. D: Biol. Crystallogr.* **2002**, *58*, 1111−1117.
(18) Cottet, M.; Faklaris, O.; Maurel, D.; Scholler, P.; Doumazane, E.; Trinquet, E.; Pin, J.-P.; Durroux, T. *Front. Endocrinol.* **2012**, *3*, 92.
(19) (a) MacManus, J. P.; Hogue, C. W.; Marsden, B. J.; Sikorska, M.; Szabo, A. G. *J. Biol. Chem.* **1990**, *265*, 10358−10366. (b) Lim, S.; Franklin, S. J. *Cell. Mol. Life Sci.* **2004**, *61*, 2184−2188. (c) Lipchik, A. M.; Parker, L. L. *Anal. Chem.* **2013**, *85*, 2582−2588.
(20) (a) Zhang, M.; Le, H. N.; Jiang, X. Q.; Yin, B. C.; Ye, B. C. *Anal. Chem.* **2013**, *85*, 11665−11674. (b) Zhang, M.; Qu, Z. B.; Ma, H. Y.; Zhou, T. S.; Shi, G. Y. *Chem. Commun.* **2014**, *50*, 4677−4679. (c) Fu, P. K. L.; Turro, C. *J. Am. Chem. Soc.* **1999**, *121*, 1−7.
(21) Chao, S. H.; Holl, M. R.; McQuaide, S. C.; Ren, T. T. H.; Gales, S. A.; Meldrum, D. R. *Opt. Express* **2007**, *15*, 10681−10689.
(22) Koga, H.; Toita, R.; Mori, T.; Tomiyama, T.; Kang, J. H.; Niidome, T.; Katayama, Y. *Bioconjugate Chem.* **2011**, *22*, 1526−1534.
(23) Wang, H. X.; Chen, W.; Xie, H. Y.; Wei, X. Y.; Yin, S. Y.; Zhou, L.; Xu, X.; Zheng, S. S. *Chem. Commun.* **2014**, *50*, 7806−7809.
(24) You, C. C.; De, M.; Han, G.; Rotello, V. M. *J. Am. Chem. Soc.* **2005**, *127*, 12873.
(25) Sun, Y.; Jiang, X.; Chen, S.; Price, B. D. *FEBS Lett.* **2006**, *580*, 4353.
(26) Dancy, B. M.; Crump, N. T.; Peterson, D. J.; Mukherjee, C.; Bowers, E. M.; Ahn, Y. H.; Yoshida, M.; Zhang, J.; Mahadevan, L. C.; Meyers, D. J.; Boeke, J. D.; Cole, P. A. *ChemBioChem* **2012**, *13*, 2113−2121.
(27) Zhang, J. H.; Chung, T. D. Y.; Oldenbury, K. R. *J. Biomol. Screening* **1999**, *4*, 67−73.

DOI: 10.1021/acs.analchem.5b01338
Anal. Chem. XXXX, XXX, XXX−XXX